Dynamic Response of a Print Belt System

The dynamic response of a print belt system, when the print belt is subjected to impulsive print forces, is analyzed in this paper. The system consists of a flat steel print belt tightly wrapped around pulleys with one of the pulleys driven by a motor. Analytical modeling allows the prediction and analysis of belt motion and thus the prediction of print misregistration. Discrete parameters used in the analysis permit simulation of the belt motion as affected by variations in belt tension, stiffness, pulley inertias, and motor-operating parameters. Conditions of belt slippage are examined, as well as the effect of dynamic loading upon the drive motor.

Introduction

An impact line printer contains basically four mechanical subsystems: a print impactor system (hammer unit), a type system, a paper system, and a ribbon system. In a belt printer the type mechanism consists of a moving belt containing engraved characters on one of its surfaces. The particular belt system of interest contains a steel belt stretched over, and supported by, a pair of pulleys. One of the pulleys that drives the belt via friction is itself driven by a motor. The flat side of the belt runs over the surface of a stationary platen, and the ribbon is between the engraved character side of the belt and the paper stack (Fig. 1). On the other side of the paper stack is the hammer unit, which is lined up along the print line with an individual hammer corresponding to each print position.

Below the engraved characters on the print belt are equally spaced raised vertical bars which act as timing marks. These timing marks are sensed by a magnetic pickup which initiates pulses that control the firing of the print hammers. A hammer is fired somewhat after the initiation of the timing pulse. A certain period of time (flight time) elapses from the firing of the hammer to the time of print impact. During impact the hammer squeezes the paper and ribbon onto the appropriate character while the belt is moving at the nominal constant belt speed. If the belt speed is changed, say due to loading, without any change in the delay time, the hammer will not squarely

impact the character. If the belt speed is changed by a large enough amount, only part of, or possibly none of, the character will be impacted, and this will result in character misregistration or partial character printing. Thus it is imperative to keep the belt velocity close to the nominal constant velocity.

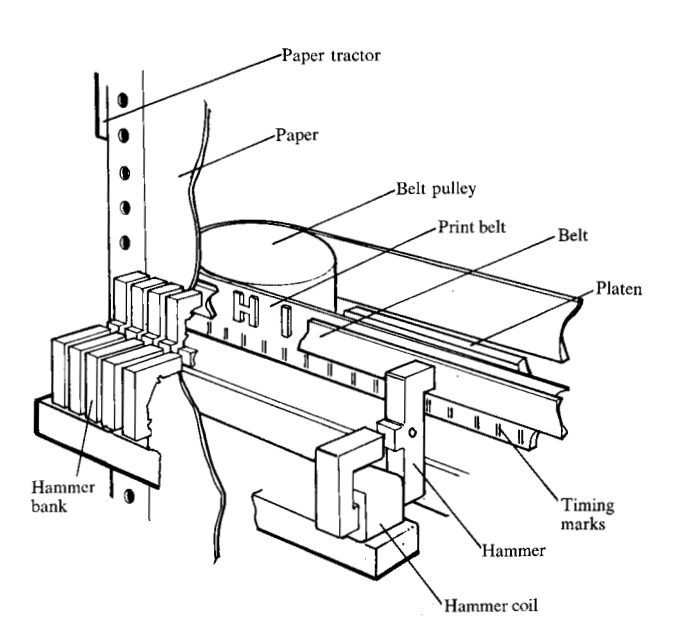
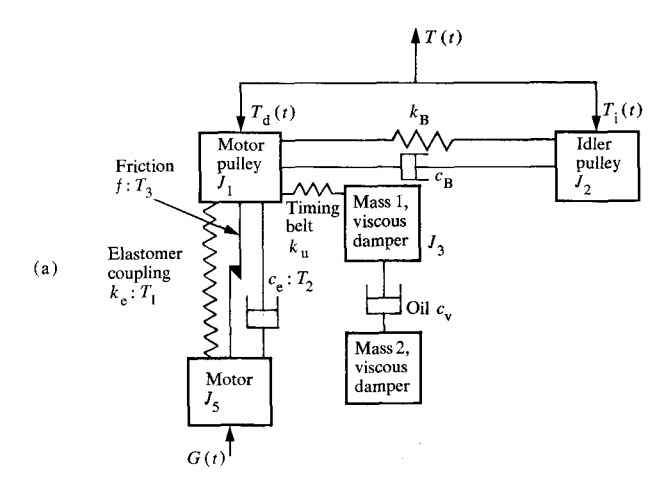


Figure 1 Belt printer.

Copyright 1979 by International Business Machines Corporation. Copying is permitted without payment of royalty provided that (1) each reproduction is done without alteration and (2) the *Journal* reference and IBM copyright notice are included on the first page. The title and abstract may be used without further permission in computer-based and other information-service systems. Permission to *republish* other excerpts should be obtained from the Editor.



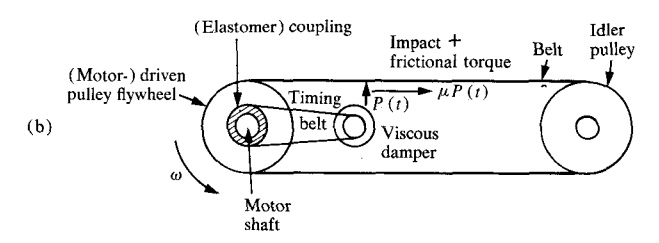


Figure 2 Representations of a belt printer mechanism: (a) printer scheme, and (b) mechanical model.

In this paper we shall analyze two effects principally responsible for altering the operational belt speed: a) belt deceleration due to printing, and b) tangential slipping of the belt against the pulleys.

The deceleration effect is due to frictional forces arising during the print cycle which adversely load down the drive motor. The drive motor adjusts to compensate for this effect by increasing its output torque with resulting velocity variations occurring. Often, external damping devices in series or in parallel with the driving motor may be employed to improve the response characteristics.

Slipping of the belt against the pulleys during printing is an effect that could also be produced by printing. Pulleys will usually be unlubricated because a high friction coefficient with the belt material is normally required. High belt tension is also required, but raising the tension poses increased stress problems throughout the printer.

To demonstrate the relative significance of belt-speed variations upon printer performance, one may note that a change of 10 cm/s in belt speed in conjunction with a print time of 1.5 ms would involve a 0.015-cm shift (misregistration) of an intended character, which is not an insignificant error.

In the following analysis, the two belt effects of deceleration and slippage are separately investigated. The results of these two analyses can then be synthesized for their total influence.

Glossary

- a_c elastomer coupler clearance
- c damping parameter
- d subscript, refers to "driver"
- E modulus of elasticity
- f coupler frictional torque
- F friction force (due to printing)
- G motor resistance torque
- i subscript, refers to "idler"
- I impulse
- J rotary moment of inertia
- k spring constant (rotational)
- K spring constant (translational)
- m mass
- P impact force
- r pulley radius
- s slip
- S belt tension
- t time
- T torque
- v belt speed
- x degrees of freedom
- θ motor lag angle
- μ coefficient of friction
- ω steady angular speed

Analysis of belt deceleration due to printing

Modeling

The mechanical system considered for analysis is fairly general, as shown in Fig. 2(a). Its main elements are a belt, a motor connected to a driver pulley, and an idler pulley. External loading (frictional impulses) is applied to the belt at some location midway between the pulleys to simulate printing.

A mechanical model of the system is shown in Fig. 2(b). Consider an excitation, in the form of frictional impulse, applied at time t=0 when the system is in a uniform steady state of motion. The displacements of inertial elements will be taken with respect to the steady state. We neglect the mass of the belt as being small compared to that of the pulleys, and we also neglect the translational motion of pulleys; thereby, a purely rotary system is assumed, where the steady counterclockwise angular speed ω is decelerated by a torque produced by printing.

Spring and dashpot elements for the belt are included in the analysis, and the motor-to-driven-pulley coupler is

considered as having stick-slip. The frictional impulse is the normal impact pulse multiplied by the Coulomb coefficient of friction. The normal impact pulse is usually measurable by force transducers built into the platen or else it can be analytically estimated. For the immediately following analysis, perfect adherence between pulleys and belt is assumed.

The motor-torque-vs-displacement characteristics were determined by quasi-static experiments on several motor types. Two eligible motor types have been considered for our study: a) stepper motor, and b) ac synchronous motor,

A bifilar-wound four-winding permanent-magnet stepper motor [1] consisting of eight stator poles and a ten-pole rotor was investigated. The step size was $\theta_{\text{step}} = 2$ deg. The torque produced by the motor with respect to the stable position $\theta = 0$ of the rotor is

$$G(\theta) \approx T_{\text{max}} \sin \frac{\pi \theta}{2\theta_{\text{step}}},$$
 (1)

where $T_{\rm max}$ is the pullout torque value depending on the angular speed ω of the rotor. The $T_{\rm max}$ vs ω relation was experimentally obtained.

When the belt printer is running in the steady state, a certain constant motor torque is required to overcome internal friction. The printload, a torque of $T(t) = \mu P(t)r$, is then applied externally. It is a fair assumption to have P(t) comprise the simultaneous contributions of all the instantaneously impacting hammers. Then, for a typical sinusoidal print pulse of n hammers hitting at equal intensity P_0 and duration t^* , we may write

$$T(t) = nr\mu P_0 \sin \frac{\pi t}{t^*}$$
 for $(0 < t < t^*)$. (2)

System equations

The five-degree-of-freedom system depicted in Fig. 2 is described by the following equations of motion:

$$\begin{split} J_{1}\ddot{x}_{1} &= k_{\rm B}(x_{2} - x_{1}) + c_{\rm B}(\dot{x}_{2} - \dot{x}_{1}) \\ &+ k_{\rm u}(x_{3} - x_{1}) - (T_{1} + T_{2} + T_{3}) + T_{\rm d}(t), \end{split} \tag{3}$$

$$J_2\ddot{x}_2 = k_{\rm B}(x_1 - x_2) + c_{\rm B}(\dot{x}_1 - \dot{x}_2) + T_{\rm i}(t), \tag{4}$$

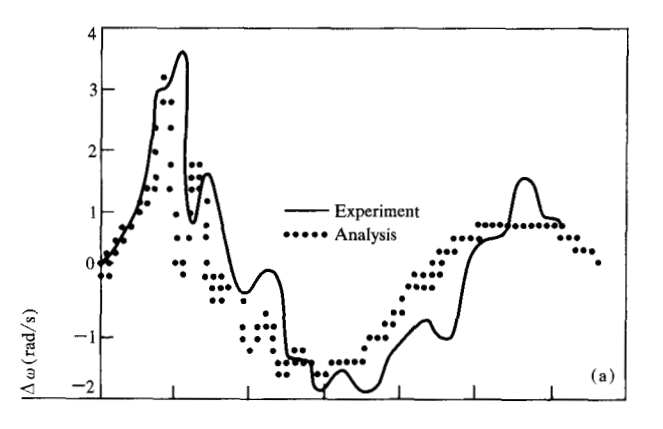
$$J_3\ddot{x}_3 = k_{\rm u}(x_1 - x_3) + c_{\rm v}(\dot{x}_4 - \dot{x}_3),\tag{5}$$

$$J_4\ddot{x}_4 = c_{\rm v}(\dot{x}_3 - \dot{x}_4),\tag{6}$$

$$J_5\ddot{x}_5 = T_1 + T_2 + T_3 - G(t), \tag{7}$$

where the contributions to the total coupling torque, between motor and driver pulley, are

$$T_1 = k_e[x_1 - x_5 - a_c \operatorname{sgn}(x_1 - x_5)]H(|x_1 - x_5| - a_c), (8)$$



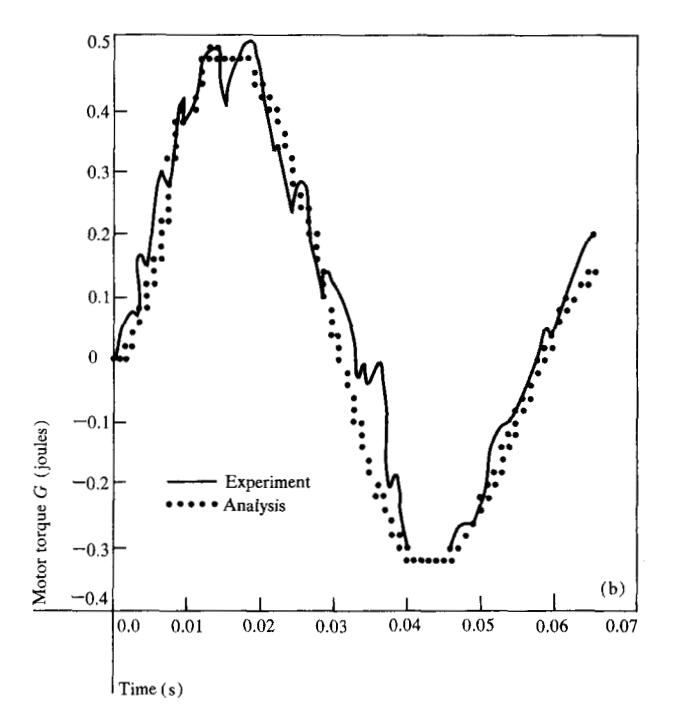
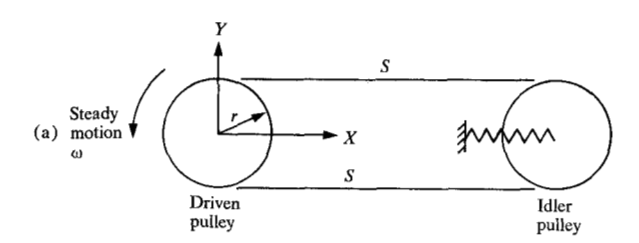


Figure 3 Typical dynamic response of print belt to a print load with stepper motor: (a) $\Delta \omega vs t$, and (b) G vs t.

$$T_2 = c_e(\dot{x}_1 - \dot{x}_s), {9}$$

$$T_3 = f \, \text{sgn} \, (\dot{x}_1 - \dot{x}_5). \tag{10}$$

In Eq. (8), H represents the Heaviside (unit) step function. For the excitation pattern of a given hammering sequence P(t), the equations of motion may be conveniently integrated using the Runge-Kutta method. The initial conditions are, in general, $\{x(t=0)\} = \{\dot{x}(t=0)\} = 0$, under the previously stated assumption that both displacements and velocities are considered as incremental quantities with respect to the steady state. With the simplifying assumption of neglecting slip over the pulleys, we may write $T_i = T_{\rm d} = T/2$. The consequences of this assump-



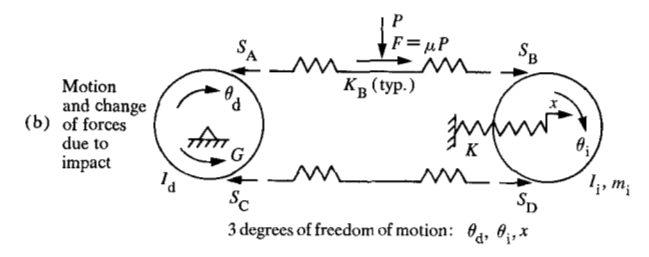


Figure 4 Model for dynamic belt response with slip.

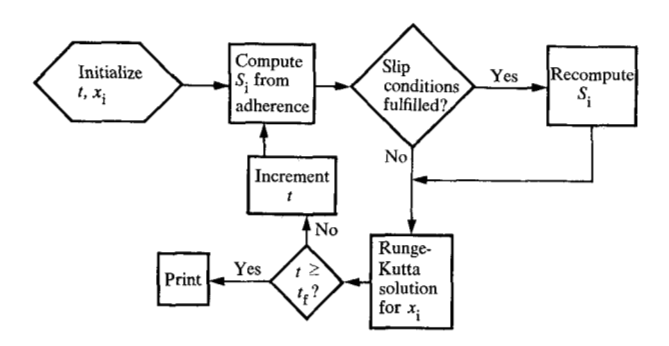


Figure 5 Flowchart for dynamic slip computation.

tion are subsequently reviewed in a later section (Analysis of belt slip) where corrected values are derived.

• Example 1—stepper motor

A belt printer driven by a stepper motor was tested. The change of velocity $\dot{\omega}$ with respect to the steady state at the motor shaft was observed by an optical transducer, and a torque measurement was incorporated in series with the motor shaft. The dynamic response to a print load was also calculated analytically.

Figure 3(a) shows the experimental and analytical variation of angular velocity change. The simultaneous change of the stepper motor torque is shown in Fig. 3(b).

Analysis of belt slip

In the previous section the deceleration of the belt due to a succession of print cycles was computed under the assumption that no slippage occurs between the belt and pulley. During any individual print cycle, however, the change of frictional forces is so sudden that the occurrence of slip must be counted upon. This will be treated presently.

Consider the belt impacted by print hammers with impact force P(t) and consequently developing potentially different tension forces in four different regions (designated by A, B, C, D) along its length. The differential tensions that are incremental to the steady-state belt tension S will be called as follows: S_A to the left of the impact, S_B to the right of it, S_C at the outlet of the motor pulley, and S_D at the inlet of the idler pulley (Fig. 4). For greater generality, the belt is considered as consisting of a series of springs K_B , and the idler pulley as having a translational spring support K in the x-direction. Altogether three degrees of freedom characterize this system: the rotations θ_d and θ_i of the driven and idler pulleys, respectively, and the translation x. The motion considered is again that of acceleration with respect to the steady-state belt motion.

The equations of motion are

$$J_{d}\ddot{\theta}_{d} = (S_{A} - S_{C})r - G, \tag{11}$$

$$J_i \ddot{\theta}_i = (S_p - S_p)r, \tag{12}$$

$$m_i \ddot{x} = -Kx - S_p - S_p, \tag{13}$$

subject to the initial conditions at t=0: $\theta_{\rm d}=\dot{\theta}_{\rm d}=\theta_{\rm i}=\dot{\theta}_{\rm i}=x=\dot{x}=0$. The incremental belt forces $S_{\rm A}$, $S_{\rm B}$, $S_{\rm C}$, $S_{\rm D}$ are those arising at locations A, B, C, D, fixed in an absolute coordinate system, not moving with the belt.

Introducing the displacements x_A , x_B , x_C , x_D at the respective points, we shall derive the relations between internal forces (S_A, \dots, S_D) and, additionally, formulate the conditions of slip. From equilibrium of the top segment of the belt we obtain

$$-S_{A} + S_{B} + F = 0. ag{14}$$

The force-displacement relation is

$$x_{\rm B} - x_{\rm A} = (S_{\rm A} + S_{\rm B})/K_{\rm B}.$$
 (15)

Similarly, for the bottom of the belt, one obtains

$$S_{\rm C} - S_{\rm D} = 0, \tag{16}$$

and

$$x_{\rm D} - x_{\rm C} = (S_{\rm C} + S_{\rm D})/K_{\rm B}.$$
 (17)

The condition of compatible displacements between belt elongation and idler pulley translation results in

$$x = (x_{\rm B} + x_{\rm D})/2. {18}$$

Assuming inextensibility of the belt over the driven pulley, we obtain

Table 1 Relations for adherence and slip. (Note: $S_D = S_C$ in each case.)

Condition	Equation characterizing the condition	$S_{\mathbf{A}}$	$S_{_{\mathbf{B}}}$	$s_{ m c}$
Adherence	Eq. (26): $x_{\rm B} - x_{\rm A} = r(\theta_{\rm i} - \theta_{\rm d}) + x$	Eq. (27): $S_A = 0.5[K_B[x + r(\theta_1 - \theta_0)] + \mu P]$	$S_{\rm B} = -S_{\rm A}$	0
Slip at driven pulley only	$\frac{\text{Eq. (28):}}{S + S_{\text{A}}} = e^{\pm \pi \mu_{\text{d}}}$	Eq. (29): $S_{A} = \frac{S(e^{\pm \pi \mu_{d}} - 1) + e^{\pm \pi \mu_{d}}(K_{B}x + \mu P/2)}{1 + e^{\pm \pi \mu_{d}}}$	by Eqs. (14), (26)	by Eqs. (22), (29)
Slip at idler pulley only	Eq. (30): $\frac{S + S_{D}}{S + S_{B}} = e^{\pm \pi \mu_{i}}$	by Eqs. (20), (31)*	by Eqs. (14), (20), (31)*	Eq. (31)*
Slip on both pulleys	Eq. (32): $\frac{S + S_A}{S + S_C} = e^{\pm \pi \mu_d}$ $\frac{S + S_D}{S + S_D} = e^{\pm \pi \mu_i}$	by Eq. (29)	by Eqs. (14), (20), (31)*	by Eq. (31)*
Slack belt	$S + S_{B}$ $\mu P = F = S_{A} - S_{B}$ Eq. (33): $S_{A} = S_{B} = S_{C} = S_{D} = -Kx/2$	by Eq. (33)	by Eq. (33)	by Eq. (33)

*Eq. (31): $S_{\rm c} = \frac{S(e^{\pm \pi \mu_1} - 1) + e^{\pm \pi \mu_1} (K_{\rm B} x - \mu P/2)}{1 + e^{\pm \pi \mu_1}}$

$$x_{A} = -x_{C}. \tag{19}$$

Note that the six equations (14)-(19) followed without excluding either motor or dynamic effects and thus should be valid for any condition of friction or slip over the pulleys. These equations yield the following useful interrelations among the eight unknown variables $(S_A, S_B, S_C, S_D; x_A, x_B, x_C, x_D)$, to be used in Eqs. (11)-(13):

$$S_{\rm A} - S_{\rm C} = 2S_{\rm A} - \frac{F}{2} - K_{\rm B}x,$$
 (20)

$$S_{\rm D} - S_{\rm B} = -2S_{\rm A} + \frac{3F}{2} + K_{\rm B}x,$$
 (21)

$$S_{\rm B} + S_{\rm D} = -\frac{F}{2} + K_{\rm B} x. \tag{22}$$

The conditions of adherence and, alternatively, of slip will now be formulated, completing the necessary computing apparatus for solving Eqs. (11)-(13). Two types of slip must be distinguished. The first type (s_1) of local slip arises when the belt slips over only one of the pulleys while the impact friction force is the Coulomb-value, $F = \mu P$. We may write for the slip velocity

$$\dot{s}_{1} = \dot{x}_{R} - \dot{x}_{A} - [r(\dot{\theta}_{1} - \dot{\theta}_{d}) + \dot{x}], \tag{23}$$

that is, the difference between elastic belt extension minus the relative displacement between tangent points A

and B of the belt. Over the slipping pulley, we shall assume that the Coulomb-condition of belt friction

$$\frac{S + S_{\text{TOP}}}{S + S_{\text{BOTTOM}}} = e^{\pm \pi \mu_{\text{i,d}}}$$
 (24)

is satisfied.

It is important to realize that, when slip is imminent over both pulleys, *i.e.*, Eq. (24) is satisfied over both pulleys, the print friction force F is no longer free to assume the value μP but will be limited to a threshold value F_2 at which total slipping (s_2) takes place. The belt is stopped cold by the printing forces for a time I, and the slip velocity is, meanwhile,

$$\dot{s}_2 \approx v.$$
 (25)

Total slipping continues until the print force diminishes below the value $P_2 = F_2/\mu$. The force $F_2 = S_{A2} - S_{B2}$, where both pairs (S_{A2}, S_{C2}) and (S_{B2}, S_{D2}) satisfy the belt friction Eq. (24).

Table 1 shows the relations characterizing various conditions of adherence and slip described above. Note that Eqs. (26)-(33) describe the mathematical handling corresponding to these conditions.

Figure 5 shows the flow diagram for the computation of the nonlinear system that necessitates a search for the

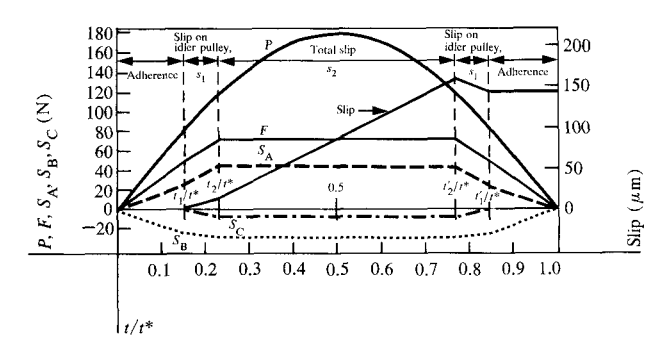


Figure 6 Belt force and slip history during single print pulse. Metal pulleys; S = 27.36 N; $\mu = 0.3 (= \mu_d = \mu_i)$.

friction conditions at every consecutive time interval, involving a step-by-step process.

Figure 6 illustrates the history of a print pulse; the belt forces S_A , S_B , $S_C = S_D$ are shown along with the print force P and friction F according to the left-hand scale. The slip is shown on the right-hand scale.

• Static approximation

Computational experience with the dynamic model just described indicated that a simplified quasi-static model would suffice in many situations (e.g., similar) to those of Example 1). Accordingly, the translational motion and the change in motor torque may be neglected as small quantities; consequently, the incremental belt forces S_A, \dots, S_D become simple functions of the instantaneous print force P.

The determination of which pulley tends to slip first is made by writing belt friction Eq. (24) for the drive pulley [Eq. (28) in Table 1] and then for the idler pulley [Eq. (30) in Table 1], since at impending slip we have

$$S_{A} = -S_{B} = \frac{\mu P}{2},$$

and

$$S_{\rm C} = S_{\rm D} = 0.$$

Both equations are solved for P, yielding $P = P_{\rm d}$ and $P = P_{\rm i}$, respectively. We thus obtain, for the print force $P_{\rm i}$ of impending slip, the choice of the smaller of the two:

$$P_{\rm d} = \frac{2S}{\mu} \ (e^{\pi\mu_{\rm d}} - 1), \tag{34}$$

and

$$P_{\rm i} = \frac{2S}{\mu} \left(\frac{e^{\pi \mu_{\rm i}} - 1}{e^{\pi \mu_{\rm i}}} \right). \tag{35}$$

The smaller of the two indicates the pulley first slipping,

at P_1 (Fig. 7). The approximate threshold impact force P_2 of total slip is obtained from satisfying both belt friction Eqs. (28) and (30), and there results

$$P_{2} = \frac{2S[(1 + e^{\pi\mu_{d}}) (e^{\pi\mu_{1}} - 1) + (1 + e^{\pi\mu_{1}}) (e^{\pi\mu_{d}} - 1)]}{\mu[1 + 2e^{\pi\mu_{1}} + e^{\pi(\mu_{1} + \mu_{d})}]}.$$
(36)

Figure 8 shows the belt forces computed by the static approximation in terms of the print force P, for two configurations of pulley friction μ and pre-tension S.

The example in Fig. 6 was solved with the static approximation, with practically identical results. The computational advantages of the approximation method are obvious since the solution of differential Eqs. (11)-(12) is now obtainable in exact form, containing only trigonometric and power terms of time.

Discussion and conclusions

The analytical description of the deceleration process in belt printers has yielded several important results. For finding the slowing down of the belt after a specified number of print impulses, it was determined (by the computer simulation) that it is often an acceptable assumption to substitute for the consecutive individual impulses I_j a constant intensity load yielding the same total impulse $I = \Sigma I_i$.

The calculations of belt response led to a five-degree-of-freedom mechanical system, and the Runge-Kutta equations were integrated sequentially. Because motor torque reaction is appreciable only after substantial lag angle has been achieved, the response calculations are time consuming; the time interval Δt used in the integration must be small enough ($\leq 100 \ \mu s$) to ensure convergence for the geometry contemplated in Example 1.

The stepper motor response was approximated by a sinusoidal expression, Eq. (1), which is of the kind usually obtained empirically. A knowledge of the dependence of $T_{\rm max}$ on phase relationships, magnetic damping, and other factors is a source of many possible engineering improvements. Both stepper motors and synchronous motors were found feasible for the printer application.

It is noted that the deceleration equations did not contain the steady belt tension S, since no slippage was assumed. The computation of slip must be carried out for an individual print pulse. Here a quasi-static approximation, neglecting translation of a pulley and motor torque resistance, may be made; but belt tension S, print force P, and the friction coefficients μ , μ_1 , and μ_d (at print-point, and over the pulleys, respectively) are crucial.

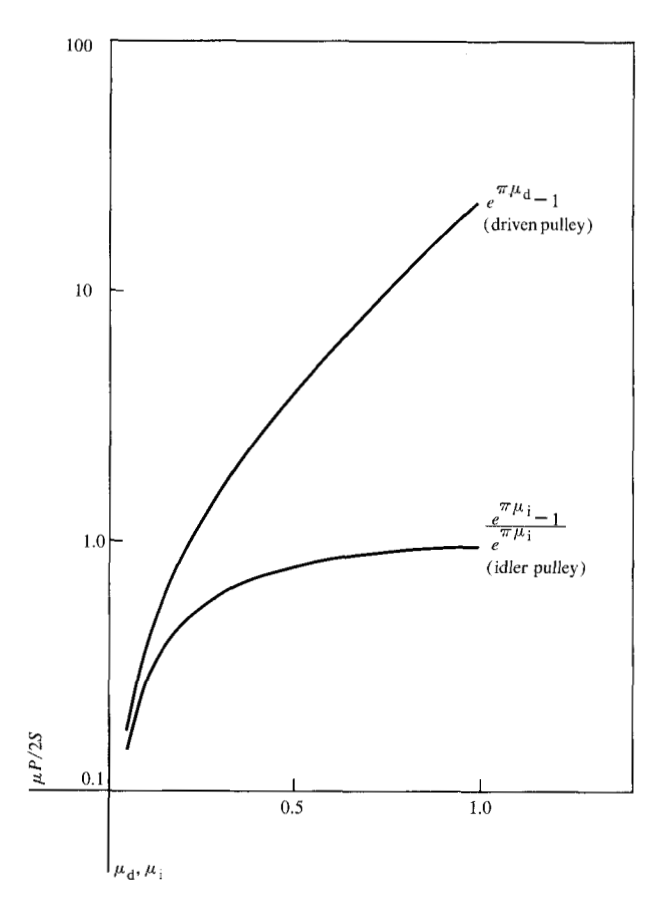


Figure 7 Curves aiding in determination of slip threshold P_1 .

Two types of slip were found to materialize. The first type of local slip (s_1) develops in the ascending phase of the print pulse when the dynamic belt tension causes slip over only one of the pulleys. However, when the print force returns to a lower value, \dot{s}_1 is zero. Local slip s_1 , at a negative rate \dot{s}_1 , can also develop in the descending phase.

The gross slip s_2 develops when the belt slips with respect to both pulleys (driven and idler). This state of affairs corresponds to the dynamic print force P reaching a value larger than P_2 , given by Eq. (36). The mathematical relationship between time and force of a pulse is assumed available; the time t_2 when P_2 is reached on the ascent of P, and the time t_2' when P reaches P_2 on the descent, straddle the gross slipping interval \bar{t} .

The net slip $s = s_2$ per print pulse can be easily expressed for a sinusoidal print pulse $P = P_0 \sin \pi t/t^*$, $(0 < t < t^*)$. We have

$$s_2 \approx v(t_2' - t_2) = v\bar{t},$$
 (37)

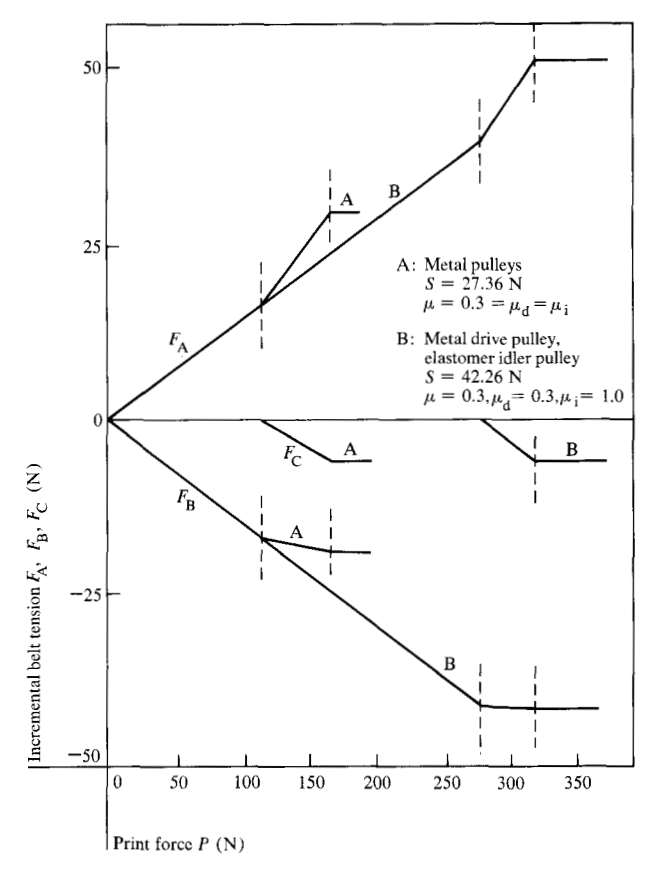


Figure 8 Static approximation of belt tension vs force of printing.

where

$$t_2 = \frac{t^*}{\pi} \arcsin \frac{P_2}{P_0},\tag{38}$$

and

$$t_{2}' = t^{*} - t_{2}. {39}$$

A nondimensional relation follows:

$$\frac{s_2}{vt^*} = 1 - \frac{2}{\pi} \arcsin \frac{P_2}{P_0}.$$
 (40)

For example, when $\mu_i = \mu_d$, we have

$$P_2 = \frac{4S}{\mu} \left(\frac{e^{\pi \mu_1} - 1}{e^{\pi \mu_1} + 1} \right),\tag{41}$$

so that the relationship between the slip, contact force, contact time, belt speed, belt tension, and the coefficients of friction can be meaningfully displayed in a graph such as in Fig. 9. It is demonstrated that the slip diminishes with increasing S, and with decreasing μ and P_0 . The pulley frictions μ_1 and μ_2 also tend to decrease the slip.

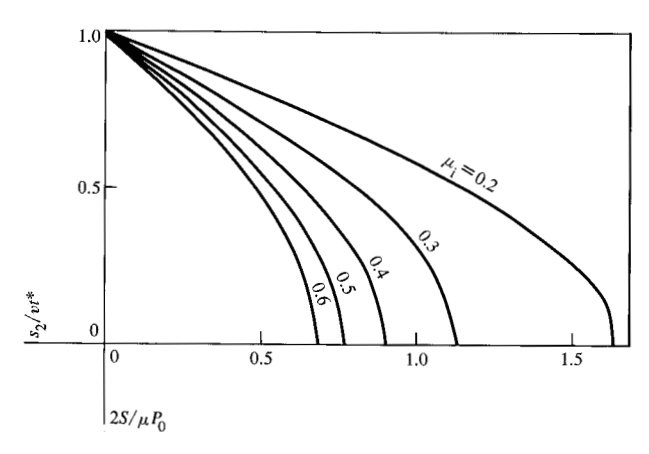


Figure 9 Nondimensional relation for gross belt slip vs belt tension, for sinusoidal print pulse when $\mu_i = \mu_d$.

It should be noted that because of gross slip, the effective print friction F cannot exceed the limit μP_2 (see Fig. 6). For this reason, only that effective frictional print torque rF ($F \le \mu P_2$), is at most decelerating the belt at any time. The frictional impulse slowing down the system

of the example in Fig. 6 is thus 20% less than that estimated from a sinusoidal print pulse $\mu P_0 \sin \pi t/t^*$. This should be considered when computing the deceleration due to a series of print pulses.

Acknowledgments

The authors thank H. C. Wang for sharing his insight on motor-printer interaction relationships. J. Mako performed experimental work on stepper motor characteristics. Torque-lag angle data for synchronous motors were determined by J. J. Lehn and H. B. Ulsh.

Reference

1. B. C. Kuo, Ed., Theory and Applications of Step Motors, West Publishing Co., New York, 1974.

Received November 31, 1978; revised February 23, 1979

The authors are located at the IBM System Products Division laboratory, P.O. Box 6, Endicott, New York 13760.